Interactive comment on “Towards accurate and practical drone-based wind measurements with an ultrasonic anemometer” by William Thielicke et al.

Anonymous Referee #1, Received and published: 21 November 2020

Dear Referee, thank you very much for taking the time to review our manuscript! We think that by incorporating your input into our manuscript (see details below), we have improved the quality and scientific significance of the paper. Here are our replies and the changes that we implemented:

1. **Little attention is paid to undisturbed flow in PBL. Include a comparison between wind lidar at higher altitudes.**
    a. Measurements in turbulent environment with a UAV appears to be most challenging to the authors, that is why we put a focus on this aspect. Data at higher altitudes (80 m and 100 m) is however included in Table 2. Flying at more than 100 m height would have required a special permit at the lidar measurement site. Additionally, the lidar data rate decreases and the measurement volume increases at altitudes > 100 m. We think that if our drone system is able to capture highly turbulent flow with small bias and RMSE, then this would only improve with altitude as the accuracy of our sonic anemometer does not depend on altitude.
2. **Discuss errors of vertical and horizontal wind component separately.**
    a. We agree that vertical and horizontal wind should be discussed separately. We implemented these changes:
        - Added Figure 10 (right) to section 3.2 showing the vertical wind component during wind tunnel testing of the full drone
        - Added the following text in section 3.2: The story is different for the wind elevation and the vertical speed. Here, the propeller induced flow has a large effect for wind speeds <= 10 m/s (see Figures 11 and 12). The wind elevation bias at very low wind speeds reaches 11°, and the vertical speed bias is around 0.4 m/s.
        - Added the column “vertical speed” in table 2, showing vertical speed bias and vertical speed RMSE in comparison the lidar measurement.
        - The conclusions do not change as the existing sentence “Propeller-induced flow mainly adds a vertical component to the flow without adding a horizontal component - even at large pitch angles. The vertical component can effectively be compensated by subtracting a value that is proportional to the mean motor throttle.” does already include a suitable statement about the vertical flow component.
3. **Test the Trisonica also on the UAV, not only in wind tunnel**
    a. The initial plan was to use the Trisonica for UAV based wind measurements, so we acquired this device. When mounted on a drone, the sensor will be tilted because of the drone’s pitch angle. Additionally, the propellers induce a vertical flow component which increases the resulting angle of attack at the sensor. During initial wind tunnel testing, we discovered that this sensor has problems to measure flows at high tilt angles. The error is not negligible and very difficult to compensate, because it also depends a lot on the yaw angle. This is why it was decided early in the design process that the accuracy will not be sufficient for the application. However, there are

already applications that use the Trisonica on a gimbal which ensures that the tilt angle is kept low. These applications will not be able to measure the vertical flow component, so measurements of the up- and downwash of a wind turbine (as presented in this paper) would not be possible. Therefore, this sensor is not suitable for our application, and consequently, we didn't test in in flight. We implemented the following change:

- Added the following sentence at the end of section 3.1: This study therefore focusses on in-flight measurements with the GILL Windmaster full-size sonic anemometer.

4. **Authors claim that the Optokopter is better than COTS platforms due to a longer flight time. Why is a long flight time advantageous? Describe advantage also in relation to statistical measures.**
    a. We do not explicitly claim that the drone is better than COTS platforms, but we are happy that the referee perceived it in this way! There are several advantages of long endurance which we admittedly did not clearly state in the manuscript: A: Figure 15 shows the advantage of long flight time. Bias and RMSE decrease with averaging interval length. The longer the averaging interval, the less data points can be measured during a single flight. B: When measuring at high altitudes, a significant portion of the flight is spent to reach the measuring location. Having a shorter flight time would at some point make measurements at high altitudes unreasonable, because the drone would spent most of the endurance for climbing and descending after an exchange of the battery. C: Discharging a lipo battery at close to 1C (which would result in 1 hr flight time) is beneficial, as high-capacity lipos should not be charged at more than 2C. Charging at 2C results in a theoretical recharge time of 30 minutes, however due to the gradual reduction of charge current at the end of the charging process, a full charge typically takes 45 minutes. With the OPTOkopter, we can therefore fly almost uninterruptedly with only two lipo batteries. Flying with a lipo as large as possible ensures that the time between these interruptions is long (45 minutes in our case). The manuscript doesn't state these advantages; therefore, we implemented these changes:
        - Updated Figure 4 with range
        - Added the following in section 2.2: When measuring at remote locations and / or at high altitude, a significant portion of the flight time is spent for reaching the measurement location. Therefore, a long flight time is beneficial, as a larger fraction of the total endurance can be spent for acquiring wind speed at the desired location. This allows for longer averaging intervals and / or more measurement locations in a single flight. Significantly less time for swapping batteries is spent during long measurement campaigns. Additionally, the drone is equipped with a dual power supply. Batteries can be swapped without cutting power of the drone, so no reboot or GNSS reacquisition is required.
5. **Describe in more detail the lessons learned: How can an existing design be optimized for most accurate wind measurements?**
    a. We have put more focus on the "lessons learned" in the update:
        - Renamed Conclusions section to Conclusions and recommendations
        - Added in conclusions: The performance of an anemometer that is to be installed on a drone should be verified at suitable tilt angles in a precision wind tunnel. The maximum tilt angle needs to be determined with drone test flights at the maximum desired wind speed.

- Added in conclusions: Placing the wind sensor far away from the rotors is a key requirement for this simple correction to work: As has been shown in Figure 6, flow distortion at the sonic anemometer is very small. This ensures that changing the pitch angle of the drone will not change the amount of flow distortion that is present at the anemometer location. In this case, a simple correction for the vertical flow component, that depends only on the average motor throttle, can be used. The gain of this correction should ideally be determined and verified in a large wind tunnel.
- Mounting an anemometer on such a long lever arm significantly increases the moment of inertia of the drone. It is therefore necessary to adjust the control loop parameters (e.g. proportional gain (P) of roll and pitch was increased by a factor of 4 and derivative gain (D) by a factor of 3). Care has to be taken to mount the anemometer exactly on top of the centre of gravity, otherwise roll and pitch motion of the drone results in an additional yaw moment. Yaw control is typically the weakest axis in quadrotors, so this could lead to serious control problems during flight. Furthermore, the anemometer mount needs to be very stiff in roll, pitch and yaw axes, otherwise oscillations (due to the increased P and D) are very likely to happen.

6. **Add information about which anemometer was used in Section 3.2 and 3.3,**
    - Added sentence in first paragraph of section 3.2: The GILL Windmaster was used as wind measuring device on the drone (see Figure 9).
    - Added sentence in first paragraph of section 3.3: After testing the performance of individual components in the measurement system, the accuracy of the full flying setup (OPTOkopter with GILL Windmaster and all compensations running) was assessed.

7. **Combine Figures 14-16**
    a. Done
8. **Combine figures 18-20**
    a. Done

Interactive comment on “Towards accurate and practical drone-based wind measurements with an ultrasonic anemometer” by William Thielicke et al.

Anonymous Referee #2, Received and published: 21 November 2020

Dear Referee, thank you very much for taking the time to review our manuscript! We think that by incorporating your input into our manuscript (see details below), we have improved the quality and scientific significance of the paper. Here are our replies and the changes that we implemented:

1. **How was data in Fig. 4 obtained? Explain.**
    a. Added the following
        - Added text in section 2.2: The relation between air speed, pitch angle and power consumption has been determined for the drone (including GILL Windmaster as shown in Figure 4 by automatically flying circles (D = 300 m) at ground speeds between 2 and 18 m/s, while logging IMU data with 10 Hz.
2. **How do accuracy and pitch angle of the sensors relate at wind speeds < 15 m/s?**
    a. The accuracy of the wind sensors have been determined for 4 pitch angles. For each pitch angle, we measured the accuracy for 36 different yaw angles (0-360 degrees). As these measurements have taken a full day per anemometer and are very expensive to do in the calibration wind tunnel, we did not perform complete pitch & yaw measurements at different wind speeds. However, we sampled different wind speeds (1, 2, 3, 5, 8, 10, 12, 15 m/s) at two different yaw angles (0° and 60°) and at zero pitch. The results show that the accuracy does not change significantly at different speed and / or yaw. We agree that measuring different pitch angles at lower speed too would be a valuable addition. However, these measurements of the isolated anemometers were mainly intended to select a suitable anemometer. We have shown in the comparison with the PTB lidar that the anemometer we selected does measure accurately at lower wind speeds / tilt angles too (as we have low bias and RMSE with long averaging intervals (see Figure 15): Wind speed bias is 3% +-1%.
3. **Comparison with wind lidar: Compare PSD of velocities measured by drone and lidar. Are there any peaks related to stabilization of the drone?**

a. We cannot detect a clear peak, respectively a distinctive peak difference in the spectrum of wind speed measurements:

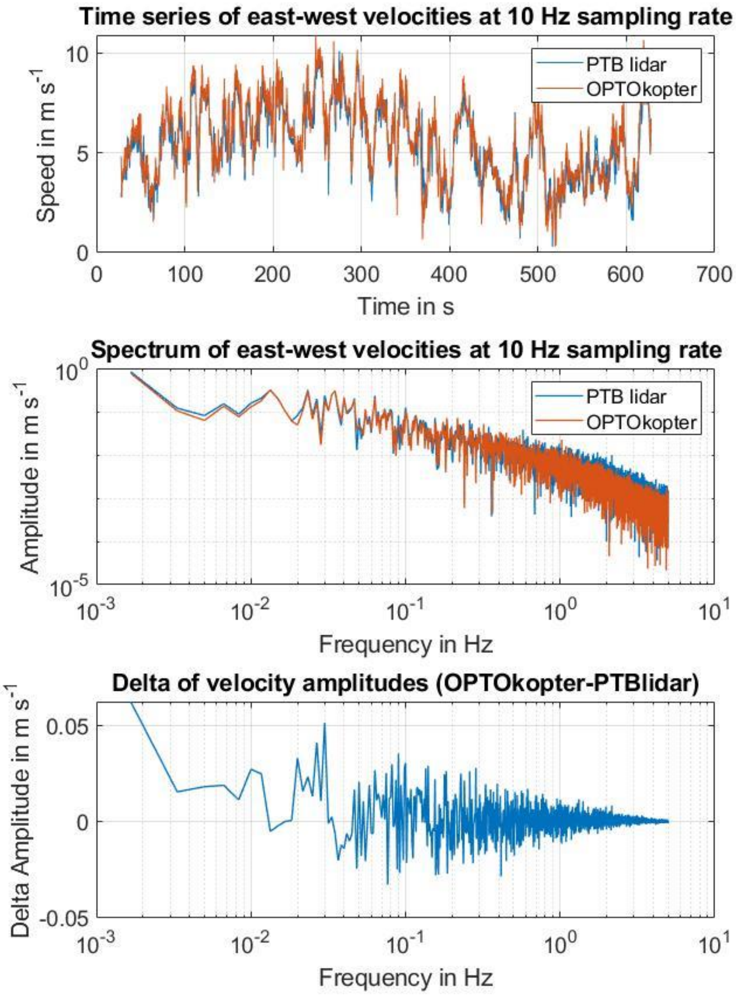

We think that most of the drone motion is effectively compensated through our compensation algorithms. This is also shown in the (updated) figure 12 (now figure 11): Erroneous wind measurements (that would result from drone motion or rotation) are suppressed with a factor of about 13. We think that the figure sufficiently shows the suppression of drone stabilization related wind measurement uncertainty.

4. **Combine figures 10 and 11**
   a. Done
5. **Combine figures 14-16**
   a. Done
6. **Combine figures 18-20**
   a. Done

Additional changes to the manuscript due to an update in the contributing authors

As the list of authors for this manuscript was updated, there are additional minor changes to the manuscript that we describe below:

1. Updated the wording so it is compatible with different parties being involved in the presented research. E.g. replaced ("We developed something" by "Something was developed").
2. The PTB lidar is validated at 8 meters height, but not at higher altitude. Therefore, using the word "validated" when presenting data at altitudes higher than 20 m is misleading. We replaced it with "analysed".
3. Updated all figures with correct axis labels (e.g. "Power [W]" replaced by "Power in W")
4. Updated Abstract: Removed "average absolute bias", as this is not comprehensible. Replaced this with a range of bias and RMSE for all the flights we performed.
5. Updated the Abstract with details on how an improved accuracy was reached:
    - "Key requirements for the accuracy are the use of a full-size sonic anemometer, a large distance between anemometer and propellers, and using a suitable algorithm for reducing the effect of propeller-induced flow."
6. Section 3.1: Instead of constantly jumping between Windmaster and Trisonica, each instrument now has its own paragraph, Trisonica is discussed first, therefore Table 1 shows the Trisonica on the left now.
7. Section 3.2: Mentioned more clearly that we used data recorded during free flight tests for setting parameters of pitch, and front / rear motor throttles in the wind tunnel:
    - "The drone was fixed to a rigid mount during most of the measurements, but using the data from normal free flight allowed to set realistic motor throttles and pitch angles for each wind tunnel speed."
8. Section 3.2: Results of the free flight inside the wind tunnel stated more clearly:
    - "This test confirmed that motor throttles and pitch angle during free wind tunnel flight and during free outside flight were in close agreement."
9. Re-worked the power spectral density plot (Figure 12 in the initial submission). Initially, we took wind speed magnitude (scalar quantity, calculated from all velocity components) for the analysis. A better approach is to directly use a velocity component. As we were oscillating in East-West direction, we took the corresponding velocity component. The resulting plot is more suitable and correct, and still shows that the motion of the drone is suppressed by a factor of about 13. The wording in all places that reference this result was adjusted accordingly.
10. Section 3.4: Removed "(within 1 m range)", as the exact (sub-second) synchronization between the timing unit in the lidar and in the drone has not been tested.
11. Section 3.4: Changes sentence about correlation of TI and RMSE to "A significant linear correlation was found also for turbulence intensity and wind speed RMSE ($r = 0.76$), azimuth RMSE ($r = 0.90$) and elevation RMSE ($r = 0.87$)."
12. Section 3.4: Replaced the "Conditions for high / low RMSE" equation with the sentence "A large distance between the measurement volumes, together with a high TI, will therefore result in high RMSE."
13. Section 3.4: Added sentence "The relative position of the OPTOkopter to the measurement volume of the lidar changed significantly while we were flying circles around the lidar. If there would be a significant influence from the OPTOkopter, then this should be visible as periodic bias error, but this is not the case."

14. Figure 16 (original Figure nr. 21), left: Did show slightly incorrect scaling, fixed
15. Conclusions: Replaced “Based on our tests of the individual components and the full system, we think that the total measurement accuracy is equal to the accuracy of the anemometer alone, as tested in the wind tunnel.” with “Based on our tests of the individual components and the full system, we think that mounting the anemometer on our drone does not significantly increase the measurement uncertainty of the anemometer.”
16. The PTB lidar data has been removed from the open data repository after a request by the PTB.

Text Compare
Produced: 04.12.2020 13:20:08

Mode: Differences, Ignoring Unimportant
Left file: \Publikation\Latex_Submission_1\Thielicke_AMT_drone_ultrasonic_v2.tex
Right file: \Publikation\Latex_Submission_2\Thielicke_AMT_drone_ultrasonic_v4.tex

Left		Right
	-+	\Author[2]{Michael}{Eggert} \Author[2]{Paul}{Wilhelm}
	-+	\affil[2]{Physikalisch-Technische Bundesanstalt, Department 1.4 Gas Flow, 38116 Braunschweig, Germany}
Wind data collection in the atmospheric boundary layer benefits from short term wind speed measurements using unmanned aerial vehicles. Fixed and rotary wing devices with diverse anemometer technology have been used in the past to provide such data, but the accuracy still has the potential to be increased. We developed a light weight drone (weight including sensor $\leq$~5~\unit{kg}) with long flight endurance (>~45~\unit{min}) for carrying an industry standard precision sonic anemometer. Accuracy tests have been performed with the isolated anemometer at high tilt angles in a calibration wind tunnel, with the drone flying in a large wind tunnel, and with the full system flying at different heights next to a bistatic lidar reference.	<>	Wind data collection in the atmospheric boundary layer benefits from short term wind speed measurements using unmanned aerial vehicles. Fixed and rotary wing devices with diverse anemometer technology have been used in the past to provide such data, but the accuracy still has the potential to be increased. A light weight drone for carrying an industry standard precision sonic anemometer was developed. Accuracy tests have been performed with the isolated anemometer at high tilt angles in a calibration wind tunnel, with the drone flying in a large wind tunnel, and with the full system flying at different heights next to a bistatic lidar reference.
The propeller-induced flow deflects the air to some extent, but this effect is compensated effectively. Our data fusion shows no signs of crosstalk between ground speed and wind speed. When compared with the bistatic lidar in very turbulent conditions, with 10~seconds averaging interval and with the UAV constantly circling around the measurement volume of the lidar reference, wind speed measurements have an average absolute bias of 1.9\% (0.073~\unit{m\,s^{-1}}), wind elevation average absolute bias is 0.5\unit{^{\circ}}, and wind azimuth average absolute bias is 1.5\unit{^{\circ}}, indicating excellent accuracy under challenging and dynamic conditions. The system was finally flown in the wake of a wind turbine, successfully measuring the spatial velocity deficit distribution during forward flight, yielding results that are in very close agreement to lidar measurements and the theoretical distribution. We believe that the results presented in this paper can provide important information for designing flying systems for precise air speed measurements either for short duration at multiple locations (battery powered) or for long duration at a single location (power supplied via cable). UAVs that are able to accurately measure three-dimensional wind might be used as cost effective and flexible addition to measurement masts and lidar scans.	<>	The propeller-induced flow deflects the air to some extent, but this effect is compensated effectively. The data fusion shows a substantial reduction of crosstalk (factor 13) between ground speed and wind speed. When compared with the bistatic lidar in very turbulent conditions, with 10~seconds averaging interval and with the UAV constantly circling around the measurement volume of the lidar reference, wind speed measurements have a bias between -2.0\% and 4.2\% (RMSE: 4.3\% to 15.5\%), vertical wind speed bias is between -0.05~\unit{m\,s^{-1}} and 0.07~\unit{m\,s^{-1}} (RMSE: 0.15~\unit{m\,s^{-1}} to 0.4~\unit{m\,s^{-1}}), elevation bias is between -1\unit{^{\circ}} and 0.7\unit{^{\circ}} (RMSE: 1.2\unit{^{\circ}} to 6.3\unit{^{\circ}}), and azimuth bias is between -2.6\unit{^{\circ}} and 7.2\unit{^{\circ}} (RMSE: 2.6\unit{^{\circ}} to 8.0\unit{^{\circ}}). Key requirements for the good accuracy under challenging and dynamic conditions are the use of a full-size sonic anemometer, a large distance between anemometer and propellers, and using a suitable algorithm for reducing the effect of propeller-induced flow.
	-+	The system was finally flown in the wake of a wind turbine, successfully measuring the spatial velocity deficit and downwash distribution during forward flight, yielding results that are in very close agreement to lidar measurements and the theoretical distribution. We believe that the results presented in this paper can provide important information for designing flying systems for precise air speed measurements either for short duration at multiple locations (battery powered) or for long duration at a single location (power supplied via cable). UAVs that are able to accurately measure three-dimensional wind might be used as cost effective and flexible addition to measurement masts and lidar scans.
\includegraphics[width=8.3cm]{figures/fig01.pdf}	<>	\includegraphics[width=8.3cm]{figures/power_curve.eps}
Power is thrust times speed, hence the power requirement of fixed-wing UAVs can be much lower than in rotary-wing UAVs at similar flight speeds (see Figure \ref{fig:fig01}). This makes fixed-wing UAVs very suitable for measuring tasks that require long flight times and large areas to be covered \citep{Thielicke2014}, especially in areas with high wind speeds that require elevated air speeds of the vehicle.	<>	Power is thrust times speed, hence the power requirement of fixed-wing UAVs can be much lower than in rotary-wing UAVs at similar flight speeds (see Fig. \ref{fig:fig01}). This makes fixed-wing UAVs very suitable for measuring tasks that require long flight times and large areas to be covered \citep{Thielicke2014}, especially in areas with high wind speeds that require elevated air speeds of the vehicle.
Due to the simplicity of deployment, the ability to measure close to structures and the potential to uninterruptedly fly the UAV via power-tethering, we decided to use a rotary wing UAV as platform. Commercial, of the shelf (COTS) wind measuring drones are not yet available. Several studies, including the ones mentioned above, use COTS drones (e.g. by companies such as DJI, 3DR, Yuneec) to carry the sensor payload. However, the flight time of a drone can only be optimized for a specific payload weight. Most COTS drones with sufficient endurance (>~30~min) are designed for larger payloads (>~1~kg) and have take-off weights easily exceeding 10~kg. We therefore designed a custom quadrotor drone around a well-proven, highly customizable, open source flight controller (ardupilot.org), enabling us to combine a custom frame with appropriate COTS electronic components and a suitable wind sensor. Keeping the total weight below 5~kg - which reduces the amount of required administrative decisions for take-off, and a long flight time (>~45~minutes) were on top of the list of requirements.	<>	Due to the simplicity of deployment, the ability to measure close to structures and the potential to uninterruptedly fly the UAV via power-tethering, a rotary wing UAV was chosen as platform. Commercial, of the shelf (COTS) wind measuring drones are not yet available. Several studies, including the ones mentioned above, use COTS drones (e.g. by companies such as DJI, 3DR, Yuneec) to carry the sensor payload. However, the flight time of a drone can only be optimized for a specific payload weight. Most COTS drones with sufficient endurance (>~30~min) are designed for larger payloads (>~1~kg) and have take-off weights easily exceeding 10~kg. Therefore, a custom quadrotor drone was designed around a well-proven, highly customizable, open source flight controller (ardupilot.org), enabling the combination of a custom frame with appropriate COTS electronic components and a suitable wind sensor. Keeping the total weight below 5~kg - which reduces the amount of required administrative decisions for take-off, and a long flight time (>~45~minutes) were on top of the list of requirements.
We identified sonic anemometers to be most suitable for the application in rotary-wing UAVs. These anemometers can sense wind from any azimuth angle from zero speed to about 50~\unit{m\,s^{-1}}. The vertical acceptance angle is up to 30\unit{^{\circ}} for some models. Rotary wing UAVs are manoeuvrable because they can move and rotate almost without restrictions in 3D space. Therefore, omnidirectional wind measurements are important to keep this benefit in manoeuvrability. Several sensors are available as COTS components, some come pre-calibrated to compensate for inbuilt shadowing effects.	<>	Sonic anemometers were identified to be most suitable for the application in rotary-wing UAVs. These anemometers can sense wind from any azimuth angle from zero speed to about 50~\unit{m\,s^{-1}}. The vertical acceptance angle is up to 30\unit{^{\circ}} for some models. Rotary wing UAVs are manoeuvrable because they can move and rotate almost without restrictions in 3D space. Therefore, omnidirectional wind measurements are important to keep this benefit in manoeuvrability. Several sensors are available as COTS components, some come pre-calibrated to compensate for inbuilt shadowing effects.
Based on the literature review presented above, we believe that special attention must be paid for the following parameters, when designing an accurate drone-based wind measuring system:	<>	Based on the literature review presented above, special attention must be paid for the following parameters, when designing an accurate drone-based wind measuring system:
The following sections describe how we analysed these parameters for our flying anemometer. We studied the 3D sensing performance of a miniature sonic anemometer and a pre-calibrated full-size sensor (with removed post to reduce weight and moment of inertia) in a calibration wind tunnel. Additionally, we analysed the influence of the propeller-induced flow by flying the UAV with attached anemometer inside a large wind tunnel. We also validated that there is no crosstalk between ground speed and wind speed during flight. The accuracy of the drone-based measurements was validated at several altitudes with a bistatic lidar. Finally, we tested the UAV in a typical measurement campaign: Wind turbine wakes are usually mapped using lidar \citep[e.g.][]{Smalikho2013,Wu2016,Herges2017}, which is relatively cost intensive and laborious. We tested the feasibility of UAV based measurements in the field by flying in the wake of a wind turbine in complex terrain.	<>	The following sections describe how these parameters were analysed for the flying anemometer. The 3D sensing performance of a miniature sonic anemometer and a pre-calibrated full-size sensor (with removed post to reduce weight and moment of inertia) was studied in a calibration wind tunnel. Additionally, the influence of the propeller-induced flow was analyzed by flying the UAV with attached anemometer inside a large wind tunnel. Subsequently, the crosstalk between ground speed and wind speed during flight was determined. The accuracy of the drone-based measurements was analysed at several altitudes with a bistatic lidar. Finally, the UAV was tested in a typical measurement campaign: Wind turbine wakes are usually mapped using lidar \citep[e.g.][]{Smalikho2013,Wu2016,Herges2017}, which is relatively cost intensive and laborious. The feasibility of UAV based measurements in the field was tested by flying in the wake of a wind turbine in complex terrain.
\includegraphics[width=4.5cm]{figures/fig03.pdf}	<>	\includegraphics[width=4.5cm]{figures/weight_breakdown.pdf}
Air speeds of up to 20~\unit{m\,s^{-1}} have been successfully tested in flight. The relation between air speed and pitch angle is shown in Figure \ref{fig:drone_properties}. A pitch angle of 30\unit{^{\circ}} is not exceeded in normal forward flight. The power consumption has a	<>	Air speeds of up to 20~\unit{m\,s^{-1}} have been successfully tested in flight.

minimum at 7~\unit{m\,s^{-1}}. With a 444~\unit{Wh} battery, we can achieve a theoretical maximum flight time of 54~minutes. In practice, only 85\% of the stored energy should be used for safety and battery lifetime reasons, which results in 46 minutes flight time.		The relation between air speed, pitch angle and power consumption has been determined for the drone (including GILL Windmaster as shown in Fig. \ref{fig:fig04}) by automatically flying circles (D = 300~m) at ground speeds between 2 and 18 ~\unit{m\,s^{-1}}, while logging IMU data with 10~\unit{Hz}. The relation between air speed and pitch angle is shown in Fig. \ref{fig:drone_properties}. A pitch angle of 30\unit{^{\circ}} is not exceeded in normal forward flight. The power consumption has a minimum at 7~\unit{m\,s^{-1}}. With a 444~\unit{Wh} battery, a theoretical maximum flight time of 54~minutes can be achieved. In practice, only 85\% of the stored energy should be used for safety and battery lifetime reasons, which results in 46 minutes flight time. When measuring at remote locations and / or at high altitude, a significant portion of the flight time is spent for reaching the measurement location. Therefore, a long flight time is beneficial, as a larger fraction of the total endurance can be spent for acquiring wind speed at the desired location. This allows for longer averaging intervals and / or more measurement locations in a single flight. Significantly less time for swapping batteries is spent during long measurement campaigns. Additionally, the drone is equipped with a dual power supply. Batteries can be swapped without cutting power of the drone, so no reboot or GNSS reacquisition is required.
Wind speed is transformed from a body-fixed reference system (BFRS) to the terrestrial reference system (TRS) using standard rotation matrices. We also compensate for the airflow induced by angular velocities in roll and pitch of the UAV. The input and output data for this transformation is given in Figure \ref{fig:fig05}. All these calculations are performed on an onboard computer (Raspberry Pi~3B+) that is getting wind speed data from the sonic anemometer at 16~Hz and attitude, position, and ground speed information from the flight controller of the UAV at 10~Hz. The onboard computer stores the measurement location in north, east, down terrestrial reference system. The wind speed vector is stored in West-East, South-North, Up-Down terrestrial reference system.	<>	Wind speed is transformed from a body-fixed reference system (BFRS) to the terrestrial reference system (TRS) using standard rotation matrices. The airflow induced by angular velocities in roll and pitch of the UAV are also compensated for. The input and output data for this transformation is given in Fig. \ref{fig:fig05}. All these calculations are performed on an onboard computer (Raspberry Pi~3B+) that is getting wind speed data from the sonic anemometer at 16~Hz and attitude, position, and ground speed information from the flight controller of the UAV at 10~Hz. The onboard computer stores the measurement location in north, east, down terrestrial reference system. The wind speed vector is stored in West-East, South-North, Up-Down terrestrial reference system.
\includegraphics[width=12cm]{figures/fig05.pdf}	<>	\includegraphics[width=12cm]{figures/fusion.pdf}
A miniature sonic anemometer \citep[TriSonica Mini Wind and Weather Sensor,][]{Anemoment2020} and a full-size, sonic anemometer \citep[factory precalibrated Windmaster,][]{Gill2020} were tested at 0~-~360\unit{^{\circ}} yaw with 0\unit{^{\circ}}, 10\unit{^{\circ}}, 20\unit{^{\circ}}, 30\unit{^{\circ}} pitch angles (see Figures \ref{fig:fig02} and \ref{fig:metas_tunnel}) in a traceable wind tunnel (400 $\cdot$ 260~mm cross-section, 400~mm length; accredited according to ISO/IEC 17025, Eidgenössisches Institut für Metrologie METAS, Switzerland) at wind speeds between 1~\unit{m\,s^{-1}} < v < 15~\unit{m\,s^{-1}}. Our measurements were compared with a calibrated propeller anemometer (measurement uncertainty 2\%) at 20\unit{^{\circ}}C, 950~hPa, 47\% humidity. Both anemometers were mounted in the wind tunnel using the same attachments as in the drone, including global navigation satellite system (GNSS) / magnetometer and cable connections to assure that measurement conditions reflect the real situation on our flying drone.	<>	A miniature sonic anemometer \citep[TriSonica Mini Wind and Weather Sensor,][]{Anemoment2020} and a full-size, sonic anemometer \citep[factory precalibrated Windmaster,][]{Gill2020} were tested at 0~-~360\unit{^{\circ}} yaw with 0\unit{^{\circ}}, 10\unit{^{\circ}}, 20\unit{^{\circ}}, 30\unit{^{\circ}} pitch angles (see Fig. \ref{fig:fig02} and \ref{fig:metas_tunnel}) in a traceable wind tunnel (400 $\cdot$ 260~mm cross-section, 400~mm length; accredited according to ISO/IEC 17025, Eidgenössisches Institut für Metrologie METAS, Switzerland) at wind speeds between 1~\unit{m\,s^{-1}} < v < 15~\unit{m\,s^{-1}}. The measurements were compared with a calibrated propeller anemometer (measurement uncertainty 2\%) at 20\unit{^{\circ}}C, 950~hPa, 47\% humidity. Both anemometers were mounted in the wind tunnel using the same attachments as in the drone, including global navigation satellite system (GNSS) / magnetometer and cable connections to assure that measurement conditions reflect the real situation on the flying drone.
\includegraphics[width=12cm]{figures/fig02.pdf}	<>	\includegraphics[width=12cm]{figures/metas_tests.pdf}
	-+	A suitable anemometer for application on UAVs should be able to accurately sense wind speed, azimuth and elevation. This should be possible for all pitch, roll and yaw angles that occur during a typical measurement flight of the UAV. In the proposed design, the maximum pitch angle of the UAV at the maximum air speed (20~\unit{m\,s^{-1}}) is 30\unit{^{\circ}}.
	-+	Wind speed measurements with the Trisonica are lower than the reference (see Table \ref{tab:tri_vs_gill}). Note that the results in Table \ref{tab:tri_vs_gill} show bias and RMSE for measurements at 15~\unit{m\,s^{-1}} and 0 - 360\unit{^{\circ}} yaw angle at four different pitch angles. At large pitch angles there is a strong bias (-17.3\% with a RMSE of 16.2\%). At zero pitch, there still is a bias of -6.3\% and a RMSE of 5.4\%. For the Trisonica, no relation between pitch angle and elevation could be determined. The Trisonica was tested in the wind tunnel in November 2018. After these results were reported to the manufacturer, a firmware update (ver 1.7.0, February 2019) addressed the issue of wind shadowing, potentially enhancing the accuracy at zero pitch angle. We had no opportunity to test this firmware in a wind tunnel yet. The issue at higher pitch angles will most likely remain, as we think it is impossible to accurately measure a vertical wind component with a small device with an inherently high blockage ratio. The latest firmware still needs to be tested in a wind tunnel for 0-360\unit{^{\circ}} and several pitch angles to check for improvements in accuracy. Based on these measurements, we think that the accuracy of 3D wind measurements with hard-mounted miniature sonic anemometers on UAVs is limited, and might explain the limited accuracy that several studies report for in-flight measurements with these kind of sensors (see Introduction). Miniature sensors should be mounted on a stabilizing gimbal and with the UAV flying at constant altitude to ensure that the vertical wind component is kept low.
A suitable anemometer for application on UAVs should be able to accurately sense wind speed, azimuth and elevation. This should be possible for all pitch, roll and yaw angles that occur during a typical measurement flight of the UAV. In our design, the maximum pitch angle of the UAV at the maximum air speed (20~\unit{m\,s^{-1}}) is 30\unit{^{\circ}}. The wind tunnel measurements of the GILL Windmaster anemometer show that bias and RMSE are small, but wind speed is overestimated by up to 3.6\% at 30\unit{^{\circ}} pitch. Note that the results in Table \ref{tab:tri_vs_gill} show bias and RMSE for measurements at 15~\unit{m\,s^{-1}} and 0 - 360\unit{^{\circ}} yaw angle at four different pitch angles. Wind speed measurements with the Trisonica are lower than the reference. At large pitch angles there is a strong bias (-17.3\% with a RMSE of 16.2\%). At zero pitch, there still is a bias of -6.3\% and a RMSE of 5.4\%. Wind azimuth sensing of the Windmaster is almost by a factor of 10 more accurate than in the Trisonica for both bias and RMSE. The Windmaster has a particularly good performance in sensing the wind elevation with a maximum bias of 1.3\unit{^{\circ}} and 1.4\unit{^{\circ}} RMSE. This is not the case for the Trisonica, where no relation between pitch angle and elevation could be determined.	<>	The wind tunnel measurements of the GILL Windmaster anemometer show that bias and RMSE are small, but wind speed is overestimated by up to 3.6\% at 30\unit{^{\circ}} pitch (see Table \ref{tab:tri_vs_gill}). Wind azimuth sensing of the Windmaster is almost by a factor of 10 more accurate than in the Trisonica for both bias and RMSE. The Windmaster has a particularly good performance in sensing the wind elevation with a maximum bias of 1.3\unit{^{\circ}} and 1.4\unit{^{\circ}} RMSE. The accuracy of this full-size sonic anemometer is well within the specs given by the manufacturer. Although it weighs by a factor of 20 more than the miniature sensor, we believe that the full-size anemometer is a more suitable instrument for the highly 3D flow on a flying and manoeuvring non-stationary UAV. This study therefore focusses on in-flight measurements with the GILL Windmaster full-size sonic anemometer.
The Trisonica was tested in the wind tunnel in November 2018. After we reported our results to the manufacturer, a firmware update (ver 1.7.0, February 2019) addressed the issue of wind shadowing, potentially enhancing the accuracy at zero pitch angle. We had no opportunity to test this firmware in a wind tunnel yet. The issue at higher pitch angles will most likely remain, as we think it is impossible to accurately measure a vertical wind component with a small device with an inherently high blockage ratio. The latest firmware still needs to be tested in a wind tunnel for 0-360\unit{^{\circ}} and several pitch angles to check for improvements in accuracy. Based on our measurements, we think that the accuracy of 3D wind measurements with hard-mounted miniature sonic anemometers on UAVs is limited, and might explain the limited accuracy that several studies report for in-flight measurements with these kind of sensors (see Introduction). Miniature sensors should be mounted on a stabilizing gimbal and with the UAV	<>	\pagebreak %otherwise content is mixed

flying at constant altitude to ensure that the vertical wind component is kept low. The accuracy of the full-size sonic anemometer is well within the specs given by the manufacturer. Although it weighs by a factor of 20 more than the miniature sensor, we believe that the full-size anemometer is a more suitable instrument for the highly 3D flow on a flying and manoeuvring non-stationary UAV.		
\pagebreak %figures are scattered throughout the text otherwise...	<>	
An anemometer that is mounted on a rotary-wing UAV is potentially measuring a velocity component that is induced by the propellers. It therefore potentially measures a biased wind speed and a biased elevation. The induced component most likely depends on the forward flight speed (air speed in this case). In normal free flight, every flight speed requires a certain pitch angle and propeller speed. We therefore determined suitable pitch angles and throttle values (voltage sag compensated) for front and rear motors by flying circles (D = 300~m) at different speeds while sampling pitch angle and motor throttle at 10~\unit{Hz} (see Figure \ref{fig:speed_throttle}). We used this data for measurements in the wind tunnel of the Technische Universität Dresden (open test section, diameter = 3~\unit{m}). Wind speeds between 1 and 19~\unit{m\,s^{-1}} were tested with the OPTOkopter being tethered to a variable pitch mount. The drone was also flown freely inside the wind tunnel to validate that the mount did not influence the measurements.	<>	An anemometer that is mounted on a rotary-wing UAV is potentially measuring a velocity component that is induced by the propellers. It therefore potentially measures a biased wind speed and a biased elevation. The induced component most likely depends on the forward flight speed (air speed in this case). In normal free flight, every flight speed requires a certain pitch angle and propeller speed. Therefore, suitable pitch angles and throttle values (voltage sag compensated) for front and rear motors were determined by flying circles (D = 300~m) at different speeds while sampling pitch angle and motor throttle at 10~\unit{Hz} (see Fig. \ref{fig:speed_throttle}). This data was used for measurements in the wind tunnel of the Technische Universität Dresden (open test section, diameter = 3~\unit{m}): The drone was fixed to a rigid mount during most of the measurements, but using the data from normal outside free flight allowed to set realistic motor throttles and pitch angles for each wind tunnel speed. Wind speeds between 1 and 19~\unit{m\,s^{-1}} were tested with the OPTOkopter being tethered to a variable pitch mount. The GILL Windmaster was used as wind measuring device on the drone (see Fig. \ref{fig:fig06}). The drone was also flown freely inside the wind tunnel to validate that the mount did not influence the measurements. This test confirmed that motor throttles and pitch angle during free wind tunnel flight and during free outside flight were in close agreement.
\includegraphics[width=8.3cm]{figures/speed_vs_throttle_pitch.pdf}	<>	\includegraphics[width=8.3cm]{figures/speed_vs_throttle_pitch.eps}
\includegraphics[width=8.3cm]{figures/fig06.pdf}	<>	\includegraphics[width=8.3cm]{figures/streamlines.pdf}
We found only little effect of the propeller flow on the measured wind speed (see Figure \ref{fig:wind_tunnel_speed}). The wind speed bias is smaller than 1.5\% for wind speeds above 5~\unit{m\,s^{-1}}. The story is different for the wind elevation, where the propeller induced flow has a large effect for wind speeds $\leq$~10~\unit{m\,s^{-1}} (see Figure~\ref{fig:wind_tunnel_vertical}). The bias at very low wind speeds reaches 11\unit{^{\circ}}. This is remarkable, because in comparison to previous studies (see Introduction), the OPTOkopter has a large distance between the anemometer and the propeller disks (1.15~m = 2.5 rotor diameters). The effect diminishes with increasing air speed, however. We compensate for this propeller induced flow using	<>	Only little effect of the propeller flow on the measured wind speed was found (see Fig. \ref{fig:wind_tunnel_all}, left). The wind speed bias is smaller than 1.5\% for wind speeds above 5~\unit{m\,s^{-1}}. The story is different for the wind elevation and the vertical speed. Here, the propeller induced flow has a large effect for wind speeds $\leq$~10~\unit{m\,s^{-1}} (see Fig.~\ref{fig:wind_tunnel_all}, middle and right). The wind elevation bias at very low wind speeds reaches 11\unit{^{\circ}}, and the vertical speed bias is around 0.4~\unit{m\,s^{-1}}. This is remarkable, because in comparison to previous studies (see Introduction), the OPTOkopter has a large distance between the anemometer and the propeller disks (1.15~m = 2.5 rotor diameters). The effect diminishes with increasing air speed, however. This propeller induced flow is compensated for using
The method keeps the bias of wind elevation below 1\unit{^{\circ}}. The effect of our compensation method is also shown in Figure \ref{fig:wind_tunnel_vertical}. To conclude, the propellers impact the direction of the flow (air is deviated downwards, which can be effectively compensated), but there is only a small influence (about 1\%) on the horizontal speed of the air, even at high pitch angles.	<>	The method keeps the bias of wind elevation below 1\unit{^{\circ}}, and the bias of the vertical wind below 0.3~\unit{m\,s^{-1}}. The effect of the compensation method is also shown in Fig. \ref{fig:wind_tunnel_all}. To conclude, the propellers impact the direction of the flow (air is deviated downwards, which can be effectively compensated), but there is only a small influence (about 1\%) on the horizontal speed of the air, even at high pitch angles.
\includegraphics[width=8.3cm]{figures/wind_tunnel_wind_speed.eps} \caption{Bias of wind speed measurements with running motors, tested in a large wind tunnel. Wind speed measurements with stopped motors are used as reference. The bias is $\leq$~1\% for wind speeds above 5~\unit{m\,s^{-1}}.} \label{fig:wind_tunnel_speed} \end{figure} \begin{figure}[!h] \includegraphics[width=8.3cm]{figures/wind_tunnel_vertical_direction.eps} \caption{Bias of elevation measurements with running motors. Measurements with stopped motors are used as reference. The simple correction algorithm limits the bias to $\leq$~1\unit{^{\circ}}.} \label{fig:wind_tunnel_vertical}	<>	\includegraphics[width=12cm]{figures/wind_tunnel_3panel.eps} \caption{Bias of wind speed (left), elevation (middle) and vertical speed (right) measurements with running motors, tested in a large wind tunnel. Wind speed measurements with stopped motors are used as reference. Wind speed bias is $\leq$~1\% for wind speeds above 5~\unit{m\,s^{-1}}. A simple correction algorithm limits the elevation bias to $\leq$~1\unit{^{\circ}}, and the vertical speed bias to $\leq$~0.3~\unit{m\,s^{-1}}, even at very high wind tunnel speed.} \label{fig:wind_tunnel_all}
\pagebreak %figures are scattered throughout the text otherwise...	<>	\pagebreak %otherwise figures appear in wrong places
After testing the performance of individual components in our measurement system, we assessed the accuracy of the full flying setup. As mentioned in the introduction, \cite{Nichols2017} report that periodic signals in the wind estimation can often be seen when a UAV is flying periodic manoeuvres and data fusion is imperfect. We checked for such problems by rapidly flying the UAV between two points that were 10 meters apart with a sinusoidal ground speed peaking at about 4~\unit{m\,s^{-1}}. Ground speed (as reported by the flight controller), air speed (as reported by the anemometer) and wind speed (as reported by our data fusion) was recorded and converted to the frequency domain using fast Fourier transform. Comparing the power spectral densities allows for evaluating the crosstalk between ground speed measurements and wind speed measurements.	<>	After testing the performance of individual components in the measurement system, the accuracy of the full flying setup (OPTOkopter with GILL Windmaster and all compensations running) was assessed. As mentioned in the introduction, \cite{Nichols2017} report that periodic signals in the wind estimation can often be seen when a UAV is flying periodic manoeuvres and data fusion is imperfect. We checked for such problems by rapidly flying the UAV between two points that were 10 meters apart in East-West direction with a sinusoidal ground speed peaking at about 4~\unit{m\,s^{-1}}. Ground speed (as reported by the flight controller), air speed (as reported by the anemometer) and wind speed (as reported by the data fusion) was recorded and converted to the frequency domain using fast Fourier transform. Comparing the amplitude spectrum allows for evaluating the crosstalk between ground speed measurements and wind speed measurements.
In a situation with zero wind, air speed and ground speed as measured by the UAV must be identical. When there is wind, these velocities will not be identical anymore. But any change in ground speed will also result in a change in air speed, hence, a spectral analysis should show peaks at the same frequencies. This is the case in our test flight (see Figure \ref{fig:pendelfft}): Both air and ground speed have a peak at 0.208~\unit{Hz}. This is the frequency that the OPTOkopter was oscillating between two waypoints. A linear regression for ground speed and air speed yields a Pearson's correlation coefficient of 0.78.	<>	In a situation with zero wind, air speed and ground speed as measured by the UAV must be identical. When there is wind, these velocities will not be identical anymore. But any change in ground speed will also result in a change in air speed, hence, a spectral analysis should show peaks at the same frequencies. This is the case in the test flight (see Fig. \ref{fig:pendelfft}): Both air and ground speed have a peak at 0.104~\unit{Hz}. This is the frequency that the OPTOkopter was oscillating between two waypoints. A linear regression for ground speed and air speed yields a Pearson's correlation coefficient of 0.944, indicating that ground speed closely relates to air speed during flight.
The FFT analysis (see Figure \ref{fig:pendelfft}) reveals, that the power spectral density of the wind speed at the relevant frequency (0.208~\unit{Hz}) is 4 to 5 orders of magnitude smaller than air speed or wind speed. Additionally, the correlation coefficient for ground speed and wind speed is 0.004. These analyses indicate that our fusion algorithm results in a wind speed measurement that is independent of ground speed and UAV motion / rotation in general. This is very important for airborne measurement systems that do not only perform point measurements in hovering flight, but are also capable of measuring while flying a mission. Such a measurement is presented in Section \ref{sect:example}.	<>	The FFT analysis (see Fig. \ref{fig:pendelfft}) reveals, that the amplitude spectrum of wind speed at the relevant frequency (0.104~\unit{Hz}) is about an order of magnitude smaller than air speed or wind speed. Additionally, the correlation coefficient for ground speed and wind speed is 0.164, indicating that there is no relevant linear relationship between these variables. These analyses indicate that the fusion algorithm results in a wind speed measurement that is mostly independent of ground speed and UAV motion / rotation in general. This is very important for airborne measurement systems that do not only perform point measurements in hovering flight, but are also capable of measuring while flying a mission. Such a measurement is presented in Section \ref{sect:example}.

\caption{Power spectral densities of ground speed, air speed and wind speed during a flight were the UAV was repeatedly oscillating between two waypoints. There is a clear peak at 0.208~\unit{Hz} in ground speed and air speed, but no peak in wind speed, indicating that wind speed measurements are not affected by the motion of the UAV.}	<>	\caption{Amplitude spectrum of ground speed (as reported by the EKF2 in the flight controller), air speed (as reported by the sonic anemometer) and wind speed (as calculated by the data fusion) during a flight were the UAV was repeatedly oscillating in East-West direction between two waypoints. There is a clear peak at 0.104~\unit{Hz} in ground speed and air speed (which corresponds to the oscillation between waypoints), but a less distinctive peak in wind speed. This indicates, that the effects on wind speed measurements caused by translation and rotation of the UAV are suppressed by a factor of 13.4 by the data fusion.}
We compared our wind measurements with the bistatic Doppler lidar, developed at the Physikalisch-Technische Bundesanstalt (PTB) in Braunschweig, Germany \citep{Oertel2019,Mauder2020}. A data output rate of 10~\unit{Hz} was used in the PTB lidar, and different heights between 20 and 100~\unit{m} were tested.	<>	We compared the drone wind measurements with the bistatic Doppler lidar, developed at the Physikalisch-Technische Bundesanstalt (PTB) in Braunschweig, Germany \citep{Oertel2019,Mauder2020}. A data output rate of 10~\unit{Hz} was used in the PTB lidar, and different heights between 20 and 100~\unit{m} were tested.
After performing several flights, we selected a measurement at 40~\unit{m} height for a detailed analysis, as the time-shift between wind speed measurements of the two methods (determined via cross-correlation) was minimal for this dataset, indicating that we were flying very close (within 1~\unit{m} range) to the measurement volume of the PTB lidar. We compared the data of the lidar reference to our measurement using an orthogonal Deming regression. RMSE and bias (based on paired observations) were determined for all measurement flights.	<>	After performing several flights, we selected a measurement at 40~\unit{m} height for a detailed analysis, as the correlation between wind speed measurements of the two methods was maximal for this dataset, indicating that we were flying very close to the measurement volume of the PTB lidar. We compared the data of the lidar reference to the drone measurement using an orthogonal Deming regression. RMSE and bias (based on paired observations) were determined for all measurement flights.
The OPTOkopter was always hovering at the lee side of the measurement volume (as indicated by a positive time-shift in the cross-correlation signal). Wind speed, azimuth and elevation were sampled during multiple short flights of 10 minutes. Additionally, we were measuring wind speeds while circling (4~\unit{m} radius, 2.5~\unit{m\,s^{-1}} flight speed) around the lidar measurement volume to check for non-zero ground-speed related errors (see Figure \ref{fig:figLidar}).	<>	The OPTOkopter was always hovering at the lee side of the measurement volume. Wind speed, azimuth and elevation were sampled during multiple short flights of 10 minutes. Additionally, we were measuring wind speeds while circling (4~\unit{m} radius, 2.5~\unit{m\,s^{-1}} flight speed) around the lidar measurement volume to check for non-zero ground-speed related errors (see Fig. \ref{fig:figLidar}).
The measurement volume of the lidar at 40~\unit{m} height is surrounded by tall buildings and trees, generating highly unsteady flow: The wind speed varies by 8~\unit{m\,s^{-1}}, the azimuth by about 100\unit{^{\circ}}, and the elevation by about 67\unit{^{\circ}} during this selected measurement flight (see Figures \ref{fig:time_resolved_ptb_magn}, \ref{fig:time_resolved_ptb_azimuth} and \ref{fig:time_resolved_ptb_elevation}). These numbers emphasize the importance of being capable to measure three-dimensional wind with a suitable anemometer. Despite the dynamic situation, the comparison with the PTB lidar reference shows an excellent agreement of the three dimensional wind speed (see Figures \ref{fig:time_resolved_ptb_magn}, \ref{fig:time_resolved_ptb_azimuth} and \ref{fig:time_resolved_ptb_elevation}). Note that these figures show measurements that were taken with 10~\unit{Hz} sampling rate. \begin{figure}[!h] \includegraphics[width=8.3cm]{figures/vergleich_kopter_lidar_time_resolved_10Hz.eps} \caption{Wind speed measurement at 10~Hz, comparison of measurement from the PTB lidar with the OPTOkopter at 40~m height. Wind speed varies between 1.5 and 9.5~\unit{m\,s^{-1}}.} \label{fig:time_resolved_ptb_magn} \end{figure}	<>	The measurement volume of the lidar at 40~\unit{m} height is surrounded by tall buildings and trees, generating highly unsteady flow: The wind speed varies by 8~\unit{m\,s^{-1}}, the azimuth by about 100\unit{^{\circ}}, and the elevation by about 67\unit{^{\circ}} during this selected measurement flight (see Fig. \ref{fig:time_resolved_ptb_all}). These numbers emphasize the importance of being capable to measure three-dimensional wind with a suitable anemometer. Despite the dynamic situation, the comparison with the PTB lidar reference shows an excellent agreement of the three dimensional wind speed (see Fig. \ref{fig:time_resolved_ptb_all}). Note that these figures show measurements that were taken with 10~\unit{Hz} sampling rate.
\includegraphics[width=8.3cm]{figures/vergleich_kopter_lidar_time_resolved_azimuth_10Hz.eps} \caption{Wind azimuth measurement at 10~Hz, comparison of measurement from the PTB lidar with the OPTOkopter at 40~m height. Wind azimuth varies between 200 and 300\unit{^{\circ}}.} \label{fig:time_resolved_ptb_azimuth} \end{figure}	+-	
\begin{figure}[!h] \includegraphics[width=8.3cm]{figures/vergleich_kopter_lidar_time_resolved_elevation_10Hz.eps} \caption{Wind elevation measurement at 10~Hz, comparison of measurement from the PTB lidar with the OPTOkopter at 40~m height. Wind elevation varies between -42 and +25\unit{^{\circ}}.} \label{fig:time_resolved_ptb_elevation}	<>	 \includegraphics[width=12cm]{figures/vergleich_kopter_lidar_time_resolved_10Hz_3panel.eps} \caption{Wind speed (left), azimuth (middle) and elevation (right) measurement at 10~Hz, comparison of measurement from the PTB lidar with the OPTOkopter at 40~m height. Wind speed varies between 1.5 and 9.5~\unit{m\,s^{-1}}. Wind azimuth varies between 200 and 300\unit{^{\circ}}. Wind elevation varies between -42 and +25\unit{^{\circ}}.} \label{fig:time_resolved_ptb_all}
A linear Deming regression of the data in 1~\unit{s} averaging intervals has a slope of 1.03 and an offset of -0.03. The correlation coefficient is 0.95, indicating a good linear relation between both methods (see Figure \ref{fig:ptb_deming}).	<>	A linear Deming regression of the data in 1~\unit{s} averaging intervals has a slope of 1.03 and an offset of -0.03. The correlation coefficient is 0.95, indicating a good linear relation between both methods (see Fig. \ref{fig:ptb_deming}).
We also analysed the effect of increasing averaging intervals (between 0.1 and 100~\unit{s}) on bias and RMSE. As expected, bias does hardly change when the averaging interval is increased. For the wind speed measurement, bias is between 2.9 and 3.7~\%, which is very similar to what we determined for the isolated Windmaster in the calibration wind tunnel (see Table \ref{tab:tri_vs_gill}). The wind speed RMSE is strongly dependent on averaging interval: It drops from 12\% at 0.1~\unit{s} to 1\% at 100~\unit{s} (see Figure \ref{fig:bias_rmse_vs_averaging_ptb_speed}).	<>	We also analysed the effect of increasing averaging intervals (between 0.1 and 100~\unit{s}) on bias and RMSE. As expected, bias does hardly change when the averaging interval is increased. For the wind speed measurement, bias is between 2.9 and 3.7~\%, which is very similar to what was determined for the isolated Windmaster in the calibration wind tunnel (see Table \ref{tab:tri_vs_gill}). The wind speed RMSE is strongly dependent on averaging interval: It drops from 12\% at 0.1~\unit{s} to 1\% at 100~\unit{s} (see Fig. \ref{fig:bias_rmse_vs_averaging_ptb_all}, left).
The azimuth has a constant bias of about 2.6\unit{^{\circ}} and a RMSE decreasing from 7\unit{^{\circ}} to 1.9\unit{^{\circ}} (see Figure \ref{fig:bias_rmse_vs_averaging_ptb_azimuth}). The offset can result from a misalignment of the lidar, or interference of the compass on the UAV. We believe that this uncertainty is acceptable. It could be improved by fusing the heading measurements of the UAV with additional sensors like dual RTK GPS rovers. The elevation bias is constantly at about 0.4\unit{^{\circ}}. RMSE decreases from 7\unit{^{\circ}} at 0.1~\unit{s} averaging interval to 1\unit{^{\circ}} at 100~\unit{s} (see Figure \ref{fig:bias_rmse_vs_averaging_ptb_elevation}).	<>	The azimuth has a constant bias of about 2.6\unit{^{\circ}} and a RMSE decreasing from 7\unit{^{\circ}} to 1.9\unit{^{\circ}} (see Fig. \ref{fig:bias_rmse_vs_averaging_ptb_all}, middle). The offset can result from a misalignment of the lidar, or interference of the compass on the UAV. We believe that this uncertainty is acceptable. It could be improved by fusing the heading measurements of the UAV with additional sensors like dual RTK GPS rovers. The elevation bias is constantly at about 0.4\unit{^{\circ}}. RMSE decreases from 7\unit{^{\circ}} at 0.1~\unit{s} averaging interval to 1\unit{^{\circ}} at 100~\unit{s} (see Fig. \ref{fig:bias_rmse_vs_averaging_ptb_all}, right).
The bistatic PTB lidar and our OPTOkopter hence give closely matched results, even at 10~\unit{Hz} sampling interval. Naturally, this consistency increases with longer averaging intervals. When measuring at slightly different locations, the influence of spatial and temporal wind speed differences decreases with longer averaging intervals, lowering RMSE. Long averaging intervals also reduce measurement noise of both methods, again decreasing RMSE.	<>	Bistatic lidar and OPTOkopter hence give closely matched results, even at 10~\unit{Hz} sampling interval. Naturally, this consistency increases with longer averaging intervals. When measuring at slightly different locations, the influence of spatial and temporal wind speed differences decreases with longer averaging intervals, lowering RMSE. Long averaging intervals also reduce measurement noise of both methods, again decreasing RMSE.
Turbulence intensity also shows a significant correlation with wind speed RMSE (r = 0.76), azimuth RMSE (r = 0.90) and elevation RMSE (r = 0.87). As a matter of course, TI also decreases when the averaging interval is increased, yielding lower RMSE (see Figures \ref{fig:bias_rmse_vs_averaging_ptb_speed}, \ref{fig:bias_rmse_vs_averaging_ptb_azimuth}, \ref{fig:bias_rmse_vs_averaging_ptb_elevation}). To conclude: \begin{itemize} \item Conditions for high RMSE: ($\upuparrows\Delta t$ \textbf{AND} $\upuparrows TI$) \textbf{OR} $\downdownarrows m_{precision}$ \item Conditions for low RMSE: ($\downdownarrows\Delta t$ \textbf{OR} $\downdownarrows TI$) \textbf{AND} $\upuparrows m_{precision}$ \item[] with Δt = time lag between measurement volumes = distance divided by mean wind speed, TI = turbulence intensity, $m_{precision}$ = measurement precision (inverse of	<>	A significant linear correlation was found also for turbulence intensity and wind speed RMSE (r = 0.76), azimuth RMSE (r = 0.90) and elevation RMSE (r = 0.87). As a matter of course, the measured TI also decreases when the averaging interval is increased, yielding lower RMSE (see Fig. \ref{fig:bias_rmse_vs_averaging_ptb_all}). A large distance between the measurement volumes, together with a high TI, will therefore result in high RMSE.

random error). \end{itemize}		
Despite sometimes we were flying very close to the lidar, we believe that the presence of the UAV did not significantly change the flow in the measurement volume of the lidar: The measurements of the OPTOkopter have been successfully compensated for propeller induced flow (see Figure \ref{fig:wind_tunnel_speed} and \ref{fig:wind_tunnel_vertical}). If the OPTOkopter would have changed e.g. the vertical flow component in the measurement volume of the lidar, then there would be a large discrepancy between (compensated) OPTOkopter measurement and (uncompensated) lidar measurement. Furthermore, measurements at more remote locations that cannot influence the measurement of the lidar due to spatial separation (see Table \ref{tab:bias_rmse_ptb_all} for bias and RMSE of all tests we performed) have a very similar bias and RMSE.	<>	Despite sometimes we were flying very close to the lidar, we believe that the presence of the UAV did not significantly change the flow in the measurement volume of the lidar: The measurements of the OPTOkopter have been successfully compensated for propeller induced flow (see Fig. \ref{fig:wind_tunnel_all}). If the OPTOkopter would have changed e.g. the vertical flow component in the measurement volume of the lidar, then there would be a large discrepancy between (compensated) OPTOkopter measurement and (uncompensated) lidar measurement. The relative position of the OPTOkopter to the measurement volume of the lidar changed significantly while we were flying circles around the lidar. If there would be a significant influence from the OPTOkopter, then this should be visible as periodic bias error, but this has not been observed in the data.
\begin{figure}[!h] \includegraphics[width=8.3cm]{figures/bias_RMSE_vs_averaging_magn.eps} \caption{Bias and RMSE of the UAV wind speed measurement at 40~\unit{m} height for averaging intervals between 0.1~\unit{s} (10~\unit{Hz}) and 100~\unit{s} (0.01~\unit{Hz}). The PTB lidar is used as reference instrument.} \label{fig:bias_rmse_vs_averaging_ptb_speed} \end{figure}	+-	
\includegraphics[width=8.3cm]{figures/bias_RMSE_vs_averaging_azimuth.eps} \caption{Bias and RMSE of the UAV wind azimuth measurement at 40~\unit{m} height for averaging intervals between 0.1~\unit{s} (10~\unit{Hz}) and 100~\unit{s} (0.01~\unit{Hz}). The PTB lidar is used as reference instrument.} \label{fig:bias_rmse_vs_averaging_ptb_azimuth} \end{figure}	+-	
\begin{figure}[!h] \includegraphics[width=8.3cm]{figures/bias_RMSE_vs_averaging_elevation.eps} \caption{Bias and RMSE of the UAV wind elevation measurement at 40~\unit{m} height for averaging intervals between 0.1~\unit{s} (10~\unit{Hz}) and 100~\unit{s} (0.01~\unit{Hz}). The PTB lidar is used as reference instrument.} \label{fig:bias_rmse_vs_averaging_ptb_elevation}	<>	\includegraphics[width=12cm]{figures/bias_RMSE_vs_averaging_3panels.eps} \caption{Bias and RMSE of the UAV wind speed (left), azimuth (middle) and elevation (right) measurement at 40~\unit{m} height for averaging intervals between 0.1~\unit{s} (10~\unit{Hz}) and 100~\unit{s} (0.01~\unit{Hz}). The PTB lidar is used as reference instrument.} \label{fig:bias_rmse_vs_averaging_ptb_all}
\caption{Bias and RMSE of the OPTOkopter wind measurements at 10~s averaging interval, with the PTB lidar reference. The table includes data from all flights that were done. The distance to the measurement volume of the lidar was difficult to assess, but it was smaller than 10~\unit{m} in all cases. The comparison was done with the OPTOkopter hovering on spot or circling around the lidar measurement volume. Wind speed bias is generally low. RMSEs seem to increase with turbulence intensity. Average absolute bias of all the measurements: wind speed 2.0\%, elevation 0.4\unit{^{\circ}}, azimuth 3.3\unit{^{\circ}}. Average absolute bias of hovering flights: wind speed 2.1\%, elevation 0.4\unit{^{\circ}}, azimuth 4.7\unit{^{\circ}}. Average absolute bias of circling flights: wind speed 1.9\%, elevation 0.5\unit{^{\circ}}, azimuth 1.5\unit{^{\circ}}.}	<>	\caption{Bias and RMSE of the OPTOkopter wind measurements at 10~s averaging interval, with the PTB lidar reference. The table includes data from all flights that were done. The distance to the measurement volume of the lidar was difficult to assess, but it was smaller than 10~\unit{m} in all cases. The comparison was done with the OPTOkopter hovering on spot or circling around the lidar measurement volume. Wind speed bias is generally low. RMSEs seem to increase with turbulence intensity.}
The wind turbine (Enercon E 70 - E 4) is located in the Black Forest in southern Germany (47°45'53.43"N; 7°51'11.68"E) at about 1012~\unit{m} above sea level. The nacelle height is 85~\unit{m} and the rotor diameter (D) is 71~\unit{m} (see Figure \ref{fig:wind_turbine_situation}). Wind velocity was determined at 2~D behind the rotor disk. Flight duration was 22~minutes, and measurements were taken at 16~\unit{Hz}. The OPTOkopter was oscillating at constant altitude at nacelle height with a velocity of 5~\unit{m\,s^{-1}} on a path parallel to the rotor disk (see Figure \ref{fig:wind_turbine_situation} and \ref{fig:turbine_flight}). Because the wind speed was quite substantially varying with time (see Figure \ref{fig:wind_turbine_reference}), all wind measurements were normalized with the reference anemometer velocity on top of the nacelle (u_{ref}). Measurements were discretized in intervals of 1~\unit{m} along the flight path. Data from each of these bins was averaged.	<>	The wind turbine (Enercon E 70 - E 4) is located in the Black Forest in southern Germany (47°45'53.43"N; 007°51'11.68"E) at about 1012~\unit{m} above sea level. The nacelle height is 85~\unit{m} and the rotor diameter (D) is 71~\unit{m} (see Fig. \ref{fig:wind_turbine_situation}). Wind velocity was determined at 2~D behind the rotor disk. Flight duration was 22~minutes, and measurements were taken at 16~\unit{Hz}. The OPTOkopter was oscillating at constant altitude at nacelle height with a velocity of 5~\unit{m\,s^{-1}} on a path parallel to the rotor disk (see Fig. \ref{fig:wind_turbine_situation} and \ref{fig:turbine_flight}). Because the wind speed was quite substantially varying with time (see Fig. \ref{fig:wind_turbine_reference}), all wind measurements were normalized with the reference anemometer velocity on top of the nacelle (u_{ref}). Measurements were discretized in intervals of 1~\unit{m} along the flight path. Data from each of these bins was averaged.
A relatively constant velocity deficit ($\overline{u}/u_{ref}$) of 25\% is found behind the full diameter of the rotor disk. Further away from the rotor tips, the velocity becomes even larger than u_{ref} (see Figure \ref{fig:turbine_wake}). Most likely, the reference anemometer is measuring velocities lower than the true free stream velocity, due to the proximity to the nacelle, and possible shadowing effects by the rotor blades. When a wind turbine rotates clockwise (as viewed from the front), it will generate a swirl with anti-clockwise rotation. In a horizontal cross-section at nacelle height, this will result in air travelling down on the left side (again viewed from the front), and air travelling up on the right side. We captured the swirl (see Figure \ref{fig:turbine_wake}, right), the magnitude is about 0.35~\unit{m\,s^{-1}} which is about 7.7\% of the average free stream velocity. The downwash is not perfectly symmetric around the centre of the wind turbine and may be influenced by the slope behind the wind turbine (see Figure \ref{fig:wind_turbine_situation}, middle).	<>	A relatively constant velocity deficit ($\overline{u}/u_{ref}$) of 25\% is found behind the full diameter of the rotor disk. Further away from the rotor tips, the velocity becomes even larger than u_{ref} (see Fig. \ref{fig:turbine_wake}). Most likely, the reference anemometer is measuring velocities lower than the true free stream velocity, due to the proximity to the nacelle, and possible shadowing effects by the rotor blades. When a wind turbine rotates clockwise (as viewed from the front), it will generate a swirl with anti-clockwise rotation. In a horizontal cross-section at nacelle height, this will result in air travelling down on the left side (again viewed from the front), and air travelling up on the right side. The swirl was captured (see Fig. \ref{fig:turbine_wake}, right), the magnitude is about 0.35~\unit{m\,s^{-1}} which is about 7.7\% of the average free stream velocity. The downwash is not perfectly symmetric around the centre of the wind turbine and may be influenced by the slope behind the wind turbine (see Fig. \ref{fig:wind_turbine_situation}, middle).
We did not capture data at $>$ 1 z/D, as the wind direction slightly changed after the waypoints were positioned and uploaded to the UAV. Our measurements are strikingly similar to theoretical velocity distributions \citep[e.g.][]{Wu2012,Keane2016} and lidar measurements in the wake of wind turbines \citep[e.g.][]{Vollmer2017,Menke2018}. We believe that the noise in the measurements is mostly due to the inconsistent free stream velocity (see Figure \ref{fig:wind_turbine_reference}) and that it can be decreased significantly by measuring for a longer duration (e.g. using more than one battery pack).	<>	Data at $>$ 1 z/D was not captured, as the wind direction slightly changed after the waypoints were positioned and uploaded to the UAV. The results of the measurements are strikingly similar to theoretical velocity distributions \citep[e.g.][]{Wu2012,Keane2016} and lidar measurements in the wake of wind turbines \citep[e.g.][]{Vollmer2017,Menke2018}. The noise in the measurements most likely results from the inconsistent free stream velocity (see Figure \ref{fig:wind_turbine_reference}) and can presumably be decreased significantly by measuring for a longer duration (e.g. using more than one battery pack).
\includegraphics[width=8.2cm]{figures/wind_turbine_flight.pdf}	<>	\includegraphics[width=8.3cm]{figures/wind_turbine_flight.pdf}
\includegraphics[width=12cm]{figures/wind_turbine_wake.pdf}	<>	\includegraphics[width=12cm]{figures/wind_turbine_wake.eps}
\conclusions %% \conclusions[modified heading if necessary] The environmental science of the atmospheric boundary layer benefits from wind speed measurements collected by UAVs. We designed a suitable light weight rotary wing UAV for carrying an anemometer. Drones can measure close to structures and they can be validated comfortably by hovering close to a reference instrument. Flight time is often an issue with UAV based measurements. In our design, the battery is responsible for 49\% of the total weight. It can be replaced by COTS power-tethering devices, that allow for much longer, uninterrupted measurement flights at a single location at different altitudes up to 100~m.	<>	\conclusions[Conclusions and recommendations] %% \conclusions[modified heading if necessary] The environmental science of the atmospheric boundary layer benefits from wind speed measurements collected by UAVs. A suitable light weight rotary wing UAV was designed for carrying an anemometer. Drones can measure close to structures and they can be validated comfortably by hovering close to a reference instrument. Flight time is often an issue with UAV based measurements. In the proposed design, the battery is responsible for 49\% of the total weight. It can be replaced by COTS power-tethering devices, that allow for much longer, uninterrupted measurement flights at a single location at different altitudes up to 100~m.
The OPTOkopter uses a full-size, industry standard anemometer instead of a miniature version, as the accuracy in three-dimensional flow is by a magnitude better. Measurements at the test site of the PTB lidar have shown that three-dimensional flow is highly likely to happen in situ, even when the OPTOkopter hovers on spot at a constant altitude. Due to the high contribution of vertical flow, using a single miniature sonic anemometer does not seem to be	<>	The OPTOkopter uses a full-size, industry standard anemometer instead of a miniature version, as the accuracy in three-dimensional flow is by a magnitude better. Measurements at the test site of the PTB lidar have shown that three-dimensional flow is highly likely to happen in situ, even when the OPTOkopter hovers on spot at a constant altitude. Due to the high contribution of vertical flow, using a single miniature sonic anemometer does not seem to be

feasible on a drone, even when the sensor is mounted on a stabilizing gimbal.		feasible on a drone, even when the sensor is mounted on a stabilizing gimbal. The performance of an anemometer that is to be installed on a drone should be verified at suitable tilt angles in a precision wind tunnel. The maximum tilt angle needs to be determined with drone test flights at the maximum desired wind speed.
Propeller-induced flow mainly adds a vertical component to the flow without adding a horizontal component - even at large pitch angles. The vertical component can effectively be compensated by subtracting a value that is proportional to the mean motor throttle. We could not find any crosstalk between ground speed and wind speed, although we were flying relatively aggressive manoeuvres (oscillating between two waypoints that were only 10~m apart). These results are supported by exceptionally low bias and RMS errors during the comparison with the bistatic PTB lidar in hovering and circling flight mode (wind speed average absolute bias = 2.0\%, elevation average absolute bias = 0.4\unit{^{\circ}}, and azimuth average absolute bias = 3.3\unit{^{\circ}}).	<>	Propeller-induced flow mainly adds a vertical component to the flow without adding a horizontal component - even at large pitch angles. The vertical component can effectively be compensated by subtracting a value that is proportional to the mean motor throttle. Placing the wind sensor far away from the rotors is a key requirement for this simple correction to work: As has been shown in Fig. \ref{fig:fig06}, flow distortion at the sonic anemometer is very small. This ensures that changing the pitch angle of the drone will not change the amount of flow distortion that is present at the anemometer location. In this case, a simple correction for the vertical flow component, that depends only on the average motor throttle, can be used. The gain of this correction should ideally be determined and verified in a large wind tunnel.
	-+	Mounting an anemometer on such a long lever arm significantly increases the moment of inertia of the drone. It is therefore necessary to adjust the control loop parameters (e.g. proportional gain (P) of the roll and pitch angular velocity controller was increased by a factor of 4 and derivative gain (D) by a factor of 3). Care has to be taken to mount the anemometer exactly on top of the centre of gravity, otherwise roll and pitch motion of the drone results in an additional yaw moment. Yaw control is typically the weakest axis in quadrotors, so this could lead to serious control problems during flight. Furthermore, the anemometer mount needs to be very stiff in roll, pitch and yaw axes, otherwise oscillations (due to the increased P and D) are very likely to happen.
	-+	The crosstalk between ground speed and wind speed is suppressed by a factor of 13, although relatively aggressive manoeuvres were flown (oscillating between two waypoints that were only 10~m apart). These results are supported by low bias and RMSE during the comparison with the bistatic lidar in hovering and circling flight mode (see Table \ref{tab:bias_rmse_ptb_all}).
Our analysis of the wind velocity in the wake of a wind turbine has proven the practicability of accurate UAV based measurements. The application is not limited to point measurements. The mean wind speed on a 200~\unit{m} long path behind the wind turbine rotor has been sampled with 1~\unit{m} resolution. Such an analysis can be executed in significantly less than an hour time including all preparations. The only requirements are a free space of 2$\cdot$2 meters for take-off and landing (e.g. the roof of a car), peak wind speeds that do not exceed 20~\unit{m\,s^{-1}}, free line of sight between pilot and UAV, and preferably no rain.	<>	The analysis of the wind velocity in the wake of a wind turbine has proven the practicability of accurate UAV based measurements. The application is not limited to point measurements. The mean wind speed on a 200~\unit{m} long path behind the wind turbine rotor has been sampled with 1~\unit{m} resolution. Such an analysis can be executed in significantly less than an hour time including all preparations. The only requirements are a free space of 2$\cdot$2 meters for take-off and landing (e.g. the roof of a car), peak wind speeds that do not exceed 20~\unit{m\,s^{-1}}, free line of sight between pilot and UAV, and preferably no rain.
Based on our tests of the individual components and the full system, we think that the total measurement accuracy is equal to the accuracy of the anemometer alone, as tested in the wind tunnel. Wind speed and elevation are sensed accurately, when data fusion is performed as described, and separation between wind sensor and propellers is large enough (here: 2.5 rotor diameters). Additionally, the maximum tilt of the drone must not exceed the maximum acceptance angle of the anemometer (30\unit{^{\circ}} in our case).	<>	Based on the tests of the individual components and the full system, we think that mounting the anemometer on the drone does not significantly increase the measurement uncertainty of the anemometer in hovering flight. Wind speed and elevation are sensed accurately, when data fusion is performed as described, and separation between wind sensor and propellers is large enough (here: 2.5 rotor diameters). Additionally, the maximum tilt of the drone must not exceed the maximum acceptance angle of the anemometer (30\unit{^{\circ}} in our case).
There certainly is room for improvement in sensing the azimuth (average absolute bias = 3.3\unit{^{\circ}}, maximum bias = 7.2\unit{^{\circ}}), which is currently limited by the magnetometer. The strongest source of interference usually are the motors of the UAV. We effectively limited this internal interference by mounting the magnetometer at a distance of 1.3~m to the motors. However, external disturbances can occur when flying close to metallic structures, which may still bias the azimuth. More accurate magnetometers recently became available for use in the Ardupilot firmware (e.g. PNI RM3100). Dual RTK GPSs or landmarks on the ground that are captured from the drone are additional possibilities to reduce azimuth bias.	<>	There certainly is room for improvement in sensing the azimuth (see Table \ref{tab:bias_rmse_ptb_all}), which is currently limited by the magnetometer. The strongest source of interference usually are the motors of the UAV. This internal interference is effectively limited by mounting the magnetometer at a distance of 1.3~m to the motors. However, external disturbances can occur when flying close to metallic structures, which may still bias the azimuth. More accurate magnetometers recently became available for use in the Ardupilot firmware (e.g. PNI RM3100). Dual RTK GPSs or landmarks on the ground that are captured from the drone are additional possibilities to reduce azimuth bias.
\dataavailability{Data of all measurements presented in this paper and additional information on the OPTOkopter are available at:	+-	
\href{https://doi.org/10.6084/m9.figshare.12581678}{https://doi.org/10.6084/m9.figshare.12581678}} %% use this section when having only data sets available	<>	\dataavailability{Data of all measurements presented in this paper (except for the PTB lidar data) and additional information on the OPTOkopter are available at: \href{https://doi.org/10.6084/m9.figshare.12581678}{https://doi.org/10.6084/m9.figshare.12581678}} %% use this section when having only data sets available
\authorcontribution{WT wrote the manuscript with input from all authors and developed the OPTOkopter together with WH. UM initiated and supported the development and assisted with all measurements that are presented. All authors contributed to the discussion of the results.} %% this section is mandatory	<>	\authorcontribution{WT wrote the manuscript with input from all authors, developed and operated the OPTOkopter together with WH. UM initiated and supported the development and assisted with all measurements that are presented. ME constructed the PTB lidar system and its signal processing. PW and ME operated the Doppler lidar and preprocessed its 10 Hz and 1 Hz raw data. All authors contributed to the discussion of the results.} %% this section is mandatory
%\disclaimer{} %% optional section	+-	
We thank the Physikalisch-Technische Bundesanstalt, Arbeitsgruppe 1.41 Stroemungsmesstechnik / Gase and especially Michael Eggert for the opportunity to compare our wind speed measurements with the bistatic lidar.	<>	We thank the Technische Universitaet Dresden, Fakultaet Maschinenwesen, Institut für Luft- und Raumfahrttechnik, Experimentelle Aerodynamik and especially Veit Hildebrand for the opportunity to fly inside the wind tunnel. Thanks to Klaus-Peter Neitzke, (Hochschule Nordhausen) and Thomas Eipper (Technische Universitaet Dresden) for the assistance with measurements and photographs during the wind tunnel flights. We thank the Eidgenössische Institut für Metrologie (METAS) for the opportunity to test the sonic anemometers in their wind tunnel. Thanks to the Ökostrom Erzeugung Freiburg GmbH, Erwin Schlauderer for allowing us to measure the wind turbine wake. Thanks to the Ardupilot community for developing a safe, great and open flight controller firmware.
We thank the Technische Universitaet Dresden, Fakultaet Maschinenwesen, Institut für Luft- und Raumfahrttechnik, Experimentelle Aerodynamik and especially Veit Hildebrand for the opportunity to fly inside the wind tunnel.	+-	
Thanks to Klaus-Peter Neitzke, (Hochschule Nordhausen) and Thomas Eipper (Technische Universitaet Dresden) for the assistance with measurements and photographs during the wind tunnel flights.	+-	
We thank the Eidgenössische Institut für Metrologie (METAS) for the opportunity to test the sonic anemometers in their wind tunnel.	+-	
Thanks to the Ökostrom Erzeugung Freiburg GmbH, Erwin Schlauderer for allowing us to measure the wind turbine wake.	+-	
Thanks to the Ardupilot community for developing a safe, great and open flight controller firmware.	+-	
\begin{thebibliography}{} \end{thebibliography}	+-	